Original Article

DOI: 10.5582/bst.2013.v7.5.237

SL1122-37, a novel derivative of sorafenib, has greater effects than sorafenib on the inhibition of human hepatocellular carcinoma (HCC) growth and prevention of angiogenesis

Yizhuo Qin[1], Yuyin Lu[1], Ruiqi Wang[1], Wenbao Li[2,*], Xianjun Qu[1,*]

[1] *Department of Pharmacology, School of Pharmaceutical Sciences, Shandong University, Ji'nan, Shandong, China;*
[2] *Sanlugen PharmaTech, Ji'nan, Shandong, China.*

Summary **SL1122-37 is a novel derivative of sorafenib that was characterized by introducing trifluoromethyl on the 4-position of indazole. We aimed to evaluate the effects of SL1122-37 on human hepatocellular carcinoma (HCC) growth and on umbilical vein vascular endothelial cells (HUVECs) angiogenesis. Its efficacy and mechanisms were compared with sorafenib. SL1122-37 significantly prevented PLC/PRF/5 cell proliferation as estimated by colorimetric assay. Flow cytometry analysis showed the induction of apoptosis and arrest of cell cycle in G1 phase. Western blotting showed the decrease of cyclin D1 and regulation of apoptotic proteins. Further analysis suggested that these effects of SL1122-37 might arise from its roles in the inhibition of multi-kinases, including c-Kit and its downstream targets and the Wnt/β-catenin pathway in PLC/PRF/5 cells. SL1122-37 also possessed the activity of antiangiogenesis, showing the prevention of HUVEC migration and capillary tube formation. Western blotting indicated the inhibition of VEGF and phosphorylation of VEGFR-2 in HUVECs. Statistical analysis suggested that SL1122-37 might possess greater activities than sorafenib in the prevention of HCC proliferation and HUVEC angiogenesis. Conclusion, SL1122-37 could develop as a potent anticancer agent for the treatment of HCC.**

Keywords: Sorafenib, SL1122-37, human hepatocellular carcinoma, multi-kinase inhibitor, antiangiogenesis

1. Introduction

Sorafenib is a multi-kinase inhibitor which is known to inhibit cancer cell proliferation by targeting Raf/MEK/ERK signaling, and to prevent angiogenesis by targeting vascular endothelial growth factor receptor tyrosine kinase. Sorafenib has shown clinical advantage in many cancers, such as hepatocellular carcinoma (HCC), breast cancer, thyroid cancer, renal cell carcinoma (RCC), and lung cancers (*1*). Sorafenib particularly exhibited benefit for the patients with advanced and unresectable HCC (*2*). However, the drug was discontinued in many patients due to severe adverse effects. The most frequent adverse events include myelosuppression, neutropenia, lymphopenia, anemia, and thrombocytopenia, hypertension and cardiovascular events, liver dysfunction, kidney injury, and abdominal pain (*3*) Although most of these adverse effects are usually manageable, myelosuppression and renal injury would led to discontinuation of treatment. Hypertension and cardiac toxicity would lead to fatal outcomes (*4*). Thus, new derivatives of sorafenib with higher activity and lower toxicity than sorafenib have remained to be investigated.

Sorafenib, N-(3-trifluoromethyl-4-chlorophenyl)-N'-(4-(2-methylcarbamoyl pyridin-4-yl)oxyphenyl)urea (Figure 1A), is structurally defined as bis-aryl ureas. Although the mechanism of sorafenib binding to its targets has remained unclear, the following analysis of its crystal structure might provide a helpful clue for designing new derivatives. Studies suggested that the carbamido in sorafenib is essential for its activity through binding with Raf protein by the formation of hydrogen bonds (*5*). After

**Address correspondence to:*
Dr. Xian-Jun Qu, Department of Pharmacology, School of Pharmaceutical Sciences, Shandong University, Ji'nan 250012, China.
E-mail: qxj@sdu.edu.cn

Dr. Wenbao Li, Sanlugen PharmaTech, Rm 506, No. 2766 Yingxiu Road, Ji'nan 250101, China.
E-mail: wbli92128@yahoo.com

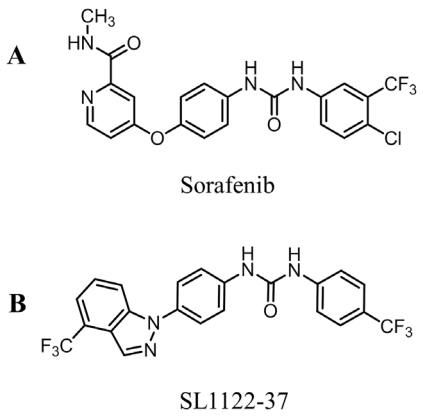

Figure 1. Chemical structures of sorafenib and SL1122-37.

binding, the distal pyridyl ring inserts into the ATP adenine binding pocket and then interacts with three aromatic residues in the hinge region, the catalytic loop, and the DFG motif. The trifluoromethyl phenyl ring at opposite end of sorafenib inserts into a hydrophobic pocket between the αC and αE helices and N-terminal regions of DFG motif and catalytic loop. These structures in sorafenib are considered to accommodate the active pockets in its targets and therefore improve the selectivity with these kinases (*6*). In our previous studies, we synthesized a series of compounds with bis-aryl ureas referenced the structure of sorafenib (*6*). In addition to the skeleton of sorafenib, these compounds contained the substituent structures of indazole or azaindazole. Our following screening assays in HCC and HUVECs indicated that some of these compounds exhibited higher activity than sorafenib. SL1122-37, 1-(4-(4-(trifluoromethyl)-1*H*-indazol-1-yl)phenyl)-3-(4-(trifluoromethyl)phenyl)urea (Figure 1B), was one of these compounds that exhibited strong activity against cancer cell proliferation and HUVEC angiogenesis. The characteristic of SL1122-37 structure is its trifluoromethyl on the 4-position of indazole. The role of trifluoromethyl in SL1122-37 might improve the electro-negativity for binding to the ATP adenine binding pocket in its target kinases. Meanwhile, the hydrogen bonds between the trifluoromethyl and the ATP adenine binding pocket could improve its activity against RAF kinase (*7*). We thus suggested that SL1122-37 might possess higher activity than sorafenib in the prevention of cancer proliferation and angiogenesis. SL1122-37 might be a promising agent that could develop as a potential agent for supplant the use of sorafenib. In this study, we evaluated the inhibitory effect of SL1122-37 on the growth of HCC cells and formation of angiogenesis in HUVECs. These effects of SL1122-37 were compared with those of sorafenib.

2. Materials and Methods

2.1. *Chemicals*

SL1122-37 as shown in Figure 1B was synthesized as described in patent (*6*). The purity of SL1122-37 as determined by high performance liquid chromatography (HPLC) was 99.9%. Sorafenib was purchased from Biochempartner China (purity 99.5%). SL1122-37 and sorafenib were dissolved in dimethylsulfoxide at 50 mM as stock solution.

2.2. *Cell lines and cell culture*

The human hepatocellular carcinoma (HCC) cells PLC/PRF/5 and umbilical vein vascular endothelial cells (HUVECs) were purchased from the American Type Culture Collection (Manassas, VA, USA). PLC/PRF/5 cells were cultured in DMEM medium supplemented with 10% heat-inactivated fetal bovine serum. HUVECs were maintained in Medium 199 supplemented with endothelial cell growth factor at 37°C in a humid atmosphere (5% CO_2-95% air). Cell proliferation was estimated by 3-[4,5-dimethylthiazol-2-yl]-2,5-diphenyltetrazolium bromide (MTT, Sigma-Aldrich, St. Louis, MO, USA) assay.

2.3. *Cell cycle analysis*

PLC/PRF/5 cells seeded in 6-well plates (1.5×10^5 per well) were synchronized by 24 h of growth in 0.5% serum medium, and then were exposed to 10% serum medium containing SL1122-37 or sorafenib for 24 h (*8*). Cells were harvested and fixed in cold 70% ethanol overnight. Cells were suspended in propidium iodide (PI) solution for 30 min. Cell cycle distribution was analyzed by using a FACScan flow cytometer (Becton Dickinson and Company, Franklin Lakes, NJ, USA).

2.4. *Annexin V/FITC/PI staining assay*

The apoptotic cells were estimated by determining the levels of phosphatidylserine on cell surface (*9*). PLC/PRF/5 cells seeded in 6-well plates (1.0×10^5 per well) were exposed to SL1122-37 or sorafenib. After exposure for 24 h, the levels of phosphatidylserine were determined by using Annexin-V/FITC and PI kit (Labtek, Dalian, Liaoning, China). The experiment was performed on a FACScan flow cytometry. The population of apoptotic cells was estimated by comparing to the vehicle control.

2.5. *Scratch assay*

The effects of SL1122-37 or sorafenib on HUVEC migration was evaluated by using a wound scratch assay. HUVECs were seeded into 6-well dish at 2.0×10^5 cells/well. Cells were allowed to attach and reach 80% confluence and a scratch (1 mm) was made through dish with a micropipette tip to generate one homogeneous wound. After wounding, the peeled off cells were removed with PBS washes. Cells were further incubated with SL1122-37 or sorafenib for 24 h and then the wound widths were measured under microscope using an ocular

grid. Cell migration = 0 time wound width (1 mm) - 24 h wound width.

2.6. *Capillary tube formation assay*

The capillary tube formation assay was performed to evaluate the activity of SL1122-37 or sorafenib against capillary tube formation of HUVECs on 3-D Matrigel. Matrigel (50 μL/per well, Becton Dickinson and Company) at 4°C was used to coat each well of a 96-well plate and then allowed to polymerize for 1 h at 37°C. Cell suspension was added to each well (2.0×10^4), together with or without SL1122-37 or sorafenib, and incubated at 37°C in a humidified chamber with 5% CO_2. The morphogenesis of capillary tube was visualized after 24 h. Images from a total of five microscopic fields per well were analyzed by Motic Image Plus 2.0 software (Motic Instruments Inc., Richmond, Canada). The tube formation was defined by counting the branch points of the formed tubes and average numbers of branch points were calculated.

2.7. *Western blotting analysis*

Cells (3.0×10^5 per well) seeded in 6-well plates were exposed to SL1122-37 or sorafenib for 24 h. Cells were harvested and cell lysates (30 μg of protein per lane) were fractionated by 10% SDS-PAGE. The proteins were electro-transferred onto nitrocellulose membranes and the protein levels were detected using the primary antibodies with appropriate dilution (*10*). The primary antibodies included those to caspase-9 (9502), caspase-3 (9662), cleaved PARP (9541), Bax (2772), cyclin D1 (2922), phospho-c-Kit (3391), c-Kit (3308), PI3K (4249), phospho-p44/42 MARK (9101), p44/42 MARK (4370), Wnt-2 (3169-1), β-catenin (9562), survivin (2808), PCNA (2586), phospho-VEGFR-2 (2478, Cell Signaling), Mcl-1 (YT2679, Immuno Way), phospho-Akt (sc-13565), Akt (sc-8312), phospho-NF-κB (sc-33020), NF-κB (sc-8008), VEGF (sc-152, Santa Cruz), c-Myc (ab32072), and β-actin (ab6276, Abcam). The bound antibodies were visualized using an enhanced chemiluminescence reagent and quantified by densitometry using ChemiDoc XRS+ image analyzer (Bio-Rad, Hercules, CA, USA). Densitometric analyses of bands were adjusted with β-actin as loading control. The percentages of increase or decrease of protein were estimated by comparison to the vehicle control (100%).

2.8. *Statistical analysis*

Data was expressed as mean ± S.D. for three different determinations. Statistical significance was analyzed by one-way analysis of variance (ANOVA) followed by Dunnett's multiple range tests. $p < 0.05$ was considered as statistically significant. Statistical analysis was performed using the SPSS/Win 13.0 software (SPSS, Inc, Chicago, IL, USA).

3. Results

3.1. *Inhibition of HCC proliferation*

PLC/PRF/5 cells were exposed to SL1122-37 or sorafenib for 72 h and then subjected to the MTT assay. As shown in Figure 2A, SL1122-37 had the similar profiles of inhibition to sorafenib, whereas a greater inhibitory effect was observed in SL1122-37 than sorafenib (0.04-1 μM, $p < 0.05$; 5 and 25 μM, $p < 0.01$ *vs*. the vehicle control). Statistical analysis indicated the difference between SL1122-37 and sorafenib (0.04-1 μM, $p < 0.05$; 5 and 25 μM, $p < 0.01$). The IC_{50} values based on the rates of inhibition at 72 h exposure in SL1122-37 and sorafenib were 4.34 and 11.39 μM, respectively.

3.2. *Arrest of cell cycle in G1 phase*

The inhibition of SL1122-37 on HCC proliferation was also determined by its activity of cell cycle arrest in G1 phase. SL1122-37 at 1.25, 2.5 and 5 μM for 24 h exposure significantly increased the population of cells with G1 phase by 25.3%, 27.6%, and 29.7%, respectively (Figure 2B c-e, $p < 0.01$ *vs*. the vehicle control). Sorafenib at 5 μM increased G1 phase cells by 10.5% (Figure 2B-b, 5 μM, $p < 0.05$ *vs*. the vehicle control). A significant difference existed between SL1122-37 and sorafenib ($p < 0.01$).

Western blotting indicated the inhibition of cyclin D1 expression in the SL1122-37- or sorafenib-treated cells. SL1122-37 at 1.25, 2.5 and 5 μM, the levels of cyclin D1 were significantly decreased by 4.1%, 51.2% and 55.5%, respectively (Figure 2C, 1.25 μM, $p > 0.05$; 2.5 and 5 μM, $p < 0.01$ *vs*. the vehicle control). Sorafenib at 5 μM reduced cyclin D1 expression by 46.1% ($p < 0.01$ *vs*. the vehicle control).

3.3. *Induction of cancer cell apoptosis*

HCC cells were analyzed by flow cytometry following staining with Annexin-V/FITC and PI. Similar profiles of cell apoptosis were observed after treatment with SL1122-37 or sorafenib. SL1122-37 at 1.25 to 5 μM for 24 h, the percentages of apoptotic cells were significantly increased to 16.1%, 24.7%, and 29.3%, respectively (Figure 3A c-e, 1.25 μM, $p < 0.05$; 2.5 and 5 μM, $p < 0.01$ *vs*. the vehicle control). Sorafenib at 5 μM induced apoptotic cells to 25.2% (Figure 3A-b, 5 μM, $p < 0.01$ *vs*. the vehicle control).

Western blotting suggested that this effect of SL1122-37 might arise from its roles in regulation of apoptotic proteins. As shown in Figure 3B, SL1122-37 at 1.25, 2.5 and 5 μM for 24 h exposure, the levels of the cleaved caspase-9 were significantly increased by 28.7%, 14.5% and 53.3%, respectively ($p < 0.01$ *vs.* the vehicle control); cleaved caspase-3 by 6.8%, 87.5% and 57.2%, respectively (1.25 μM, $p > 0.05$; 2.5 and 5 μM, $p < 0.01$ *vs*. the vehicle control); cleaved PARP by 20.2%, 287.5% and 350.5%,

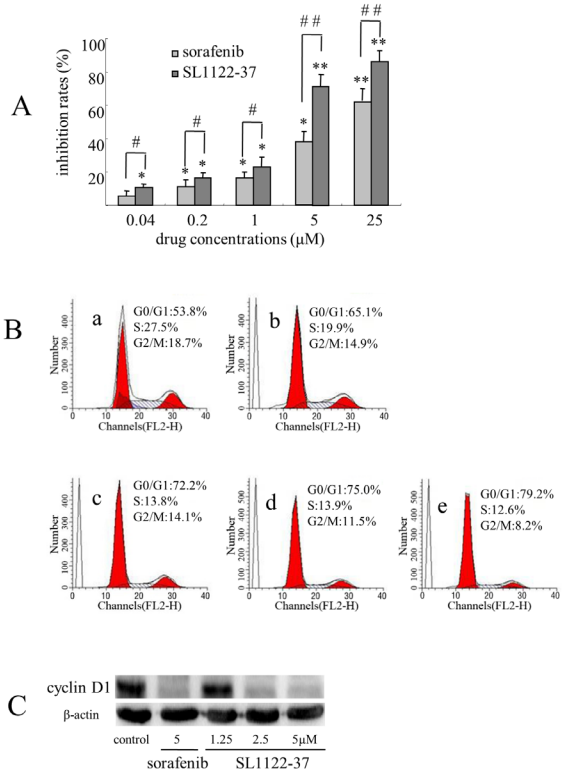

Figure 2. The effects of SL1122-37 on PLC/PRF/5 proliferation. (A) The inhibition of PLC/PRF/5 proliferation was estimated by the MTT assay. *$p < 0.05$, **$p < 0.01$ *vs*. the vehicle control. #$p < 0.05$, ##$p < 0.01$ between SL1122-37 and sorafenib. **(B)** SL1122-37 arrested cell cycle in G1 phase as determined by a FACS-can flow cytometer. **a**: the vehicle control; **b**: sorafenib 5 μM; **c-e**: SL1122-37 1.25, 2.5 and 5 μM, respectively. **(C)** Western blotting showed the inhibition of cyclin D1 expression by SL1122-37 or sorafenib. Western blotting assay was performed as described in the Materials and methods. Densitometric analyses of bands were adjusted with β-actin as loading control. The percentages of decrease of protein were estimated by comparison to the vehicle control (100%). The bars indicated mean ± S.D. ($n = 3$).

respectively (1.25 μM, $p < 0.05$; 2.5 and 5 μM, $p < 0.01$ *vs*. the vehicle control). While the levels of pro-caspase-9, pro-caspase-3 were consequently decreased, respectively. Further analysis indicated the increase of Bax and decrease of Mcl-1 in the SL1122-37-treated cells. The ratio of Bax/Mcl-1 was significantly increased as compared with the vehicle control (Figure 3B, 1.25 μM, $p < 0.05$; 2.5 and 5 μM, $p < 0.01$ *vs*. the vehicle control). Sorafenib at 5 μM increased the level of the cleaved caspase-9 by 36.8% ($p < 0.05$ *vs*. the vehicle control); cleaved caspase-3 by 10.5% ($p > 0.05$ *vs*. the vehicle control); and cleaved PARP by 278.2% ($p < 0.01$ *vs*. the vehicle control), respectively. A significant difference existed between SL1122-37 and sorafenib (5 μM, $p < 0.05$).

3.4. *Inhibition of a multiple tyrosine kinase activity in HCC cells*

Western blotting analysis determined the levels of the multi-kinases in PLC/PRF/5 cells. Both sorafenib and SL1122-37 had the activity of modulating the expression of these tyrosine kinases, whereas SL1122-37 possessed more potential than sorafenib. SL1122-37 at 1.25, 2.5 and 5 μM for 24 h exposure prevented phosphor-c-Kit expression by 6.4%, 46.1%, and 88.2%, respectively (Figure 4A, $p < 0.01$ *vs*. the vehicle control); PI3K by 5.8%, 29.1%, 57.3%, respectively (2.5 μM, $p < 0.05$; 5 μM, $p < 0.01$ *vs*. the vehicle control); phospho-Akt by 3.4%, 28.6%, 82.9%, respectively (2.5 μM, $p < 0.05$; 5 μM, $p < 0.01$ *vs*. the vehicle control); phospho-ERK1/2 by 26.2%, 65.6%, 84.5%, respectively (1.25 μM, $p < 0.05$; 2.5 and 5 μM, $p < 0.01$ *vs*. the vehicle control) (Figure 4B); NF-κB by 13.2%, 30.3%, 89.9%, respectively (2.5 μM, $p < 0.05$; 5 μM, $p < 0.01$ *vs*. the vehicle control); phospho-NF-κB by 16.4%, 26.7%, 72.7%, respectively

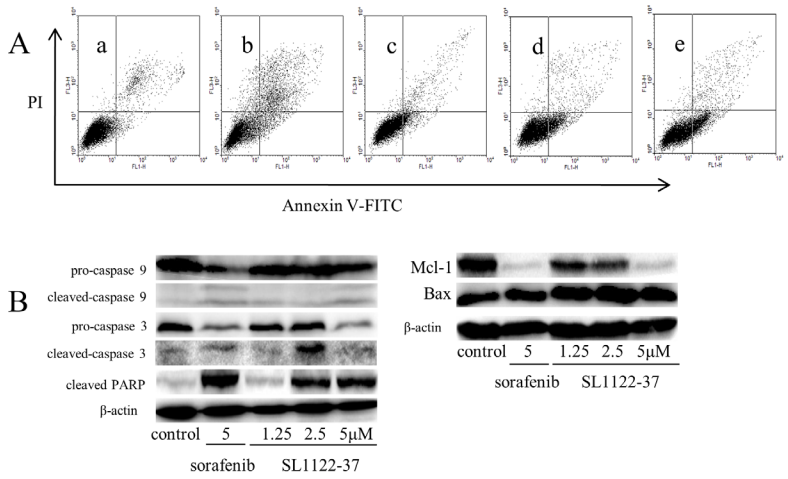

Figure 3. SL1122-37 or sorafenib induced PLC/PRF/5 cells to apoptosis. (A) Flow cytometry analyzed the apoptotic cells exposed to 5 μM of sorafenib (**b**) or different concentrations of SL1122-37 for 24 h (**a**, the vehicle control; **c-e**, 1.25, 2.5 and 5 μM, respectively). **(B)** Western blotting analyzed the changes of apoptotic proteins in PLC/PRF/5 cells. The procedure was described as Figure 2. The ratio of Bax/Mcl-1 was calculated by dividing the density value of Bax by that of Mcl-1 at same point. Triplicate experiments were performed with triplicate samples.

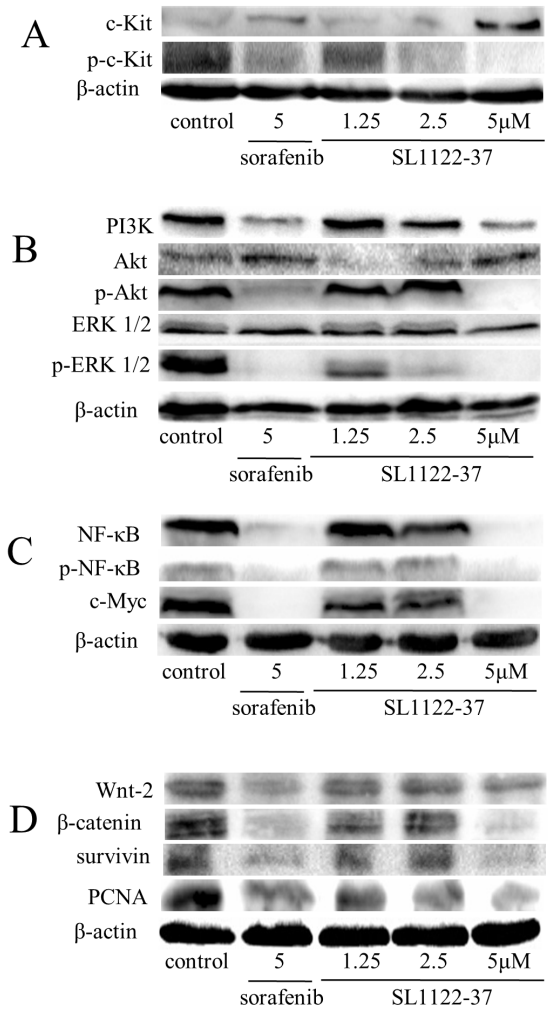

Figure 4. Western blotting analysis demonstrated the inhibition of multi-kinases and modulation of the Wnt/β-catenin pathway in PLC/PRF/5 cells exposed to SL1122-37 or sorafenib. Western blotting assay was performed as described in Figure 2. Densitometric analyses of bands were adjusted with β-actin as loading control. The percentages of decrease or increase of protein were estimated by comparison to the vehicle control (100%). Triplicate experiments were performed separately.

(2.5 μM, $p < 0.05$; 5 μM, $p < 0.01$ *vs*. the vehicle control); c-Myc by 10.6%, 25.9%, 89.7%, respectively (1.25 and 2.5 μM, $p < 0.05$; 5 μM, $p < 0.01$ *vs*. the vehicle control) (Figure 4C). Sorafenib at 5 μM reduced the level of phosphor-c-Kit by 35.5%, PI3K by 40.8%, phospho-Akt by 18.4%, phospho-ERK1/2 by 67.2%, NF-κB by 69.4%, phospho-NF-κB by 72.6%, c-Myc by 79.9% ($p < 0.01$ *vs*. the vehicle control). The comparative analysis of these data indicated that SL1122-37 had greater activity than sorafenib in the modulation of these kinases ($p < 0.05$ between SL1122-37 and sorafenib).

3.5. *Modulation of the Wnt/β-catenin signaling pathway*

We evaluated the activity of SL1122-37 in the modulation of the Wnt/β-catenin pathway. As shown in Figure 4D, SL1122-37 at 1.25, 2.5 and 5 μM significantly reduced the level of Wnt-2 expression by 11.6%, 30.4% and 49.8%, respectively (1.25 and 2.5 μM, $p < 0.05$; 5 μM, $p < 0.01$ *vs*. the vehicle control); β-catenin by 31.6%, 39.0% and 81.9%, respectively (1.25 and 2.5 μM, $p < 0.05$; 5 μM, $p < 0.01$ *vs*. the vehicle control); PCNA by 36.6%, 55.0%, and 75.9%, respectively (1.25 μM, $p < 0.05$; 2.5 and 5 μM, $p < 0.01$ *vs*. the vehicle control); survivin by 25.0%, 44.3%, and 59.8%, respectively (1.25 and 2.5 μM, $p < 0.05$; 5 μM, $p < 0.01$ *vs*. the vehicle control). Sorafenib at 5 μM inhibited the level of Wnt-2 expression by 36.9% ($p < 0.05$ *vs*. the vehicle control); β-catenin by 65.4% ($p < 0.01$ *vs*. the vehicle control); PCNA by 37.0% ($p < 0.05$ *vs*. the vehicle control); survivin by 47.9% ($p < 0.05$ *vs*. the vehicle control), respectively. Statistic analysis showed the significant difference between SL1122-37 and sorafenib (survivin, $p < 0.05$; Wnt-2, β-catenin and PCNA, $p < 0.01$).

3.6. *Prevention of angiogenesis in HUVECs*

Figure 5A showed the similar profiles of SL1122-37 and sorafenib in the inhibition of HUVECs growth. SL1122-37 at 0.04 and 0.2 μM did not obviously inhibit HUVECs proliferation ($p > 0.05$ *vs*. the vehicle control), whereas SL1122-37 at the concentrations range from 1 to 25 μM, the inhibition of HUVECs was significantly increased by 17.6%, 36.8%, and 79.3%, respectively (1 μM, $p < 0.05$; 5 and 25 μM, $p < 0.01$ *vs*. the vehicle control). Sorafenib at the same concentrations inhibited HUVEC proliferation by 12.0%, 21.8%, and 59.9%, respectively (1 and 5 μM, $p < 0.05$; 25 μM, $p < 0.01$ *vs*. the vehicle control). A significant difference was seen between SL1122-37 and sorafenib at the range from 1 μM to 25 μM ($p < 0.05$).

The prevention of HUVEC migration by SL1122-37 or sorafenib was then determined (Figure 5B). HUVECs in the control group exhibited highly spontaneous migration. The average spontaneous distance at 24 h incubation was 620 μm. The ability of migration was markedly reduced in the presence of SL1122-37 or sorafenib. The migration distances of HUVEC exposure to 1.25, 2.5 and 5 μM of SL1122-37 were 228, 146 and 87 μm, respectively ($p < 0.01$ *vs*. the vehicle control). The migration distances of HUVEC exposure to the same concentrations of sorafenib were 388, 263 and 157 μm, respectively ($p < 0.05$ *vs*. the vehicle control). Statistical analysis of these data showed the difference between SL1122-37 and sorafenib ($p < 0.05$).

SL1122-37 possessed the activity against capillary tube formation and this activity was greater than sorafenib. As shown in Figure 5C, the branch points of capillary tube in the vehicle control cells were 27 (26.6 ± 3.8). SL1122-37 at 1.25, 2.5 and 5 μM for 24 h exposure, the number of branch points were significantly reduced to 16 (by 40%), 15 (by 42.5%) and 9 (by 67.5%), respectively (1.25 μM, $p < 0.05$; 2.5 and 5 μM, $p < 0.01$ *vs*. the vehicle control). Sorafenib by 5 μM reduced the branch points of capillary tube to 14 (47.3%) (Figure 5C-b, $p < 0.05$ *vs*. the vehicle control).

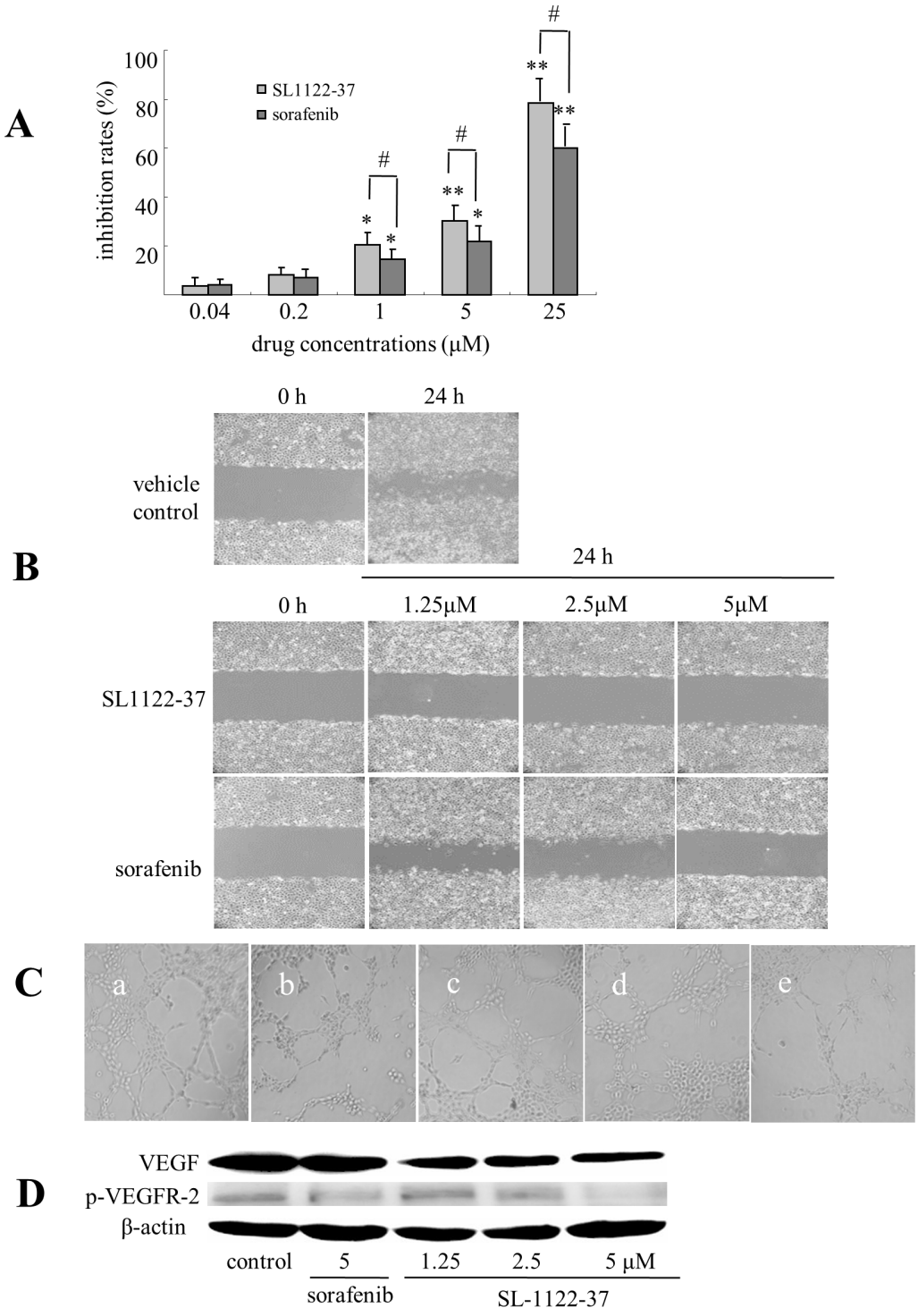

Figure 5. The effects of SL1122-37 on HUVECs. (A) The inhibition of cell growth was estimated by the MTT assay. The bars indicated mean ± S.D. (n = 3). *p < 0.05, **p < 0.01 *vs*. the vehicle control. #p < 0.05 between SL1122-37 and sorafenib. **(B)** The inhibition of HUVECs migration by SL1122-37 or sorafenib as determined by the scratch assay. Cell migration = 0 time wound width (1 mm) - 24 h wound width. **(C)** The prevention of HUVEC tube formation on 3-D Matrigel, **a**: vehicle control; **b**: sorafenib 5 μM; **c-e**: SL1122-37 1.25, 2.5 and 5 μM, respectively. **(D)** Western blotting showed the inhibition of VEGF and phosphor-VEGFR-2 in HUVECs exposed to SL1122-37 or sorafenib. Triplicate experiments were performed separately.

There was a significant difference between SL1122-37 and sorafenib (p < 0.05).

Western blotting determined the levels of VEGF and phospho-VEGF receptor 2 in HUVECs (Figure 5D). SL1122-37 at 1.25, 2.5 and 5 μM reduced the levels of VEGF by 38.8%, 57.7%, and 79.9%, respectively (1.25 μM, p < 0.05; 2.5 and 5 μM, p < 0.01 *vs*. the vehicle control); phospho-VEGF receptor 2 by 22.3%, 53.0%, and 81.8%, respectively (1.25 and 2.5 μM, p < 0.05; 5 μM, p < 0.01 *vs*. the vehicle control). Sorafenib at 5 μM reduced the level of VEGF expression by 21.5% (p < 0.05 *vs*. the vehicle control); phospho-VEGF receptor 2 by 30.9% (p

< 0.05 *vs*. the vehicle control), respectively. Significant differences existed between SL1122-37 and sorafenib ($p < 0.05$).

4. Discussion

In this study, we determined the inhibitory effects of SL1122-37, a novel derivative of sorafenib, on the proliferation of HCC PLC/PRF/5 cells and the formation of angiogenesis of HUVECs. Its efficacy and mechanisms were compared with those of sorafenib. SL1122-37 possessed the activity against cancer cell proliferation. We suggested that these high effects of SL1122-37 might arise from its roles in the apoptotic induction and regulation of cell cycle. The mechanisms of SL1122-37 action might associate with its activity in the inhibition of multi-kinases. The following assays were performed to determine its activity of antiangiogenesis. SL1122-37 strongly prevented HUVECs migration and capillary tube formation. The activity of SL1122-37 against angiogenesis was greater than sorafenib. The effect of antiangiogenesis might be due to the prevention of VEGF and phospho-VEGFR in HUVECs. These results support our strategy of designing new derivatives based on sorafenib.

Studies showed that the inhibition of sorafenib on cancer growth was mainly due to its activity of apoptotic induction (*11*). Sorafenib might induce cancer cells to apoptosis through activating the intrinsic mitochondria-mediated pathway (*12*). Further studies suggested that the crucial event for initiating this pathway might due to its role in the inhibition of myeloid cell leukemia-1 (Mcl-1) (*13*). As a member of the antiapoptotic Bcl-2 family, Mcl-1 is overexpressed in HCC. Overexpression of Mcl-1 could protect cancer cells from apoptosis. Down-regulation of Mcl-1 is related to the release of cytochrome c from mitochondria into cytosol, caspase activation, and apoptotic cell death. The Bax/Mcl-1 ratio has thus been considered to be a marker of apoptosis activation (*14*). In this study, SL1122-37 was found to have the similar profiles in the inhibition of HCC and induction of apoptosis, whereas its activities were more potential than sorafenib. We thus suggested that SL1122-37 might induce cancer cells to apoptosis through initiating the intrinsic mitochondria-mediated pathway.

RAF/mitogen-activated protein/extracellular signal-regulated kinase (ERK) kinase (MEK)/ERK cascade signaling pathway has been considered to play crucial roles in the development of HCC (*15*). In this pathway, the activation of c-Kit might be an important initial event. Activated c-Kit could regulate the transcription of its multiple downstream targets, such as the Ras-Raf-MEK-ERK cascade and PI3K/Akt pathway. The cytoplasmic target of ERK and Akt is IKK (*16*). Activation of IKK leads to the degradation of IκB, resulting in the translocation of NF-κB into nucleus and transcription of targeted genes. High level of NF-κB has been implicated in the regulation of apoptosis, proliferation and c-Myc expression (*17*). We evaluated the activity of SL1122-37 against these kinases and compared them with those of sorafenib. SL1122-37 possessed the similar profiles against these kinases, whereas its effect was greater than sorafenib. We thus suggested that SL1122-37 might be a promising multi-kinase inhibitor.

The high efficacy of SL1122-37 might also be contributed by its roles in the modulation of the Wnt/β-catenin pathway. Over-expression of the Wnt/β-catenin pathway is frequently observed in HCC. Activation of Wnt-2 and β-catenin has been considered to be the initial events for HCC proliferation (*18*). Its downstream targets, such as cyclin D1, survivin, PCNA and c-Myc, are consequently amplified following the initial event (*19*). Among these targets, PCNA is a marker of cell proliferation and is highly expressed during G1 and S phases. Cyclin D1 is a cell cycle protein frequently overexpressed in HCC. High level of c-Myc could stimulate cancer growth and prevent them from apoptosis. Survivin is an anti-apoptotic molecule widely expressed in HCC. Overexpression of survivin leads to antiapoptosis (*20*). In this study, SL1122-37 was observed to have a greater activity than sorafenib in modulation of this pathway, suggesting its roles in the inhibition of HCC.

HCC is a hypervascular tumor and the progression of invasion is highly correlated to the formation of angiogenesis (*21*). Angiogenesis actually starts with vascular endothelial cells and cancerous tumor cells releasing molecules. These signals activate the proliferation and migration of vascular endothelial cells leading to endothelial cell sprouts in stromal space. The crucial signal of angiogenesis is the release of vascular endothelial growth factor (VEGF). Circulating VEGF binds to its receptors (VEGFR1-3, mainly 2) on endothelial cells and induces the dimerization and autophosphorylation of the receptor, which activates the downstream signal eventually leading to angiogenesis (*16*). Using HUVECs, SL1122-37 was found to have a greater inhibitory effect than sorafenib on the angiogenesis. This effect might arise from its roles in the inhibition of VEGF and its autophosphorylation of the receptors. These results support our strategy of designing SL1122-37 to be an angiogenesis inhibitor. However, more evidence of antiangiogenesis and mechanisms of action are needed.

In summary, SL1122-37 possessed greater activity than sorafenib in the inhibition HCC growth and HUVECs angiogenesis. These inhibitory effects of SL1122-37 might arise from its roles in the induction of apoptosis and inhibition of multiple kinases. We suggested that SL1122-37 might be a promising compound that could be developed as a potential agent for the treatment of HCC.

Acknowledgements

This project was supported by the Ministry of Science and Technology of China (2010ZX09401-302-2-07 and 2011ZX09102-001-03).

References

1. Wilhelm S, Carter C, Lynch M, Lowinger T, Dumas J, Smith RA, Schwartz B, Simantov R, Kelley S. Discovery and development of sorafenib: A multikinase inhibitor for treating cancer. Nat Rev Drug Discov. 2006; 5:835-844.
2. Waghray A, Balci B, El-Gazzaz G, Kim R, Pelley R, Narayanan Menon K, Estfan B, Romero-Marrero C, Aucejo F. Safety and efficacy of sorafenib for the treatment of recurrent hepatocellular carcinoma after liver transplantation. Clin Transplant. 2013; 27:555-561.
3. Wu S, Chen JJ, Kudelka A, Lu J, Zhu X. Incidence and risk of hypertension with sorafenib in patients with cancer: a systematic review and meta-analysis, Incidence and risk of hypertension with sorafenib in patients with cancer: A systematic review and meta-analysis. Lancet Oncol. 2008; 9:117-123.
4. Veronese ML, Mosenkis A, Flaherty KT, Gallagher M, Stevenson JP, Townsend RR, O'Dwyer PJ. Mechanisms of hypertension associated with BAY 43-9006. J Clin Oncol. 2006; 24:1363-1369.
5. Wan PT, Garnett MJ, Roe SM, Lee S, Niculescu-Duvaz D, Good VM, Jones CM, Marshall CJ, Springer CJ, Barford D, Marais R. Mechanism of activation of the RAF-ERK signaling pathway by oncogenic mutations of B-RAF. Cell. 2004; 116:855-867.
6. Li WB. The design and synthesze of anti-cancer agent belong to indazole or azaindazole based diarylureas or diarylsulfoureas, China patent (2012), CN 102153551B.
7. Zhu T, Jiao Y, Chen YD, Wang X, Li HF, Zhang LY, Lu T. Pharmacophore identification of Raf-1 kinase inhibitors. Bioorg Med Chem Lett. 2008; 18:2346-2350.
8. Cui CZ, Wen XS, Cui M, Gao J, Sun B, Lou HX. Synthesis of solasodine glycoside derivatives and evaluation of their cytotoxic effects on human cancer cells. Drug Discov Ther. 2012; 6:9-17.
9. Bommareddy A, Zhang XY, Kaushik RS, Dwivedi C. Effects of components present in flaxseed on human colon adenocarcinoma Caco-2 cells: Possible mechanisms of flaxseed on colon cancer development in animals. Drug Discov Ther. 2010; 4:184-189.
10. Zamri N, Masuda N, Oura F, Yajima Y, Nakada H, Fujita-Yamaguchi Y. Effects of two monoclonal antibodies, MLS128 against Tn-antigen and 1H7 against insulin-like growth factor-I receptor, on the growth of colon cancer cells. Biosci Trends. 2012; 6:303-312.
11. Sun NK, Huang SL, Chang TC, Chao CC. Sorafenib induces endometrial carcinoma apoptosis by inhibiting Elk-1-dependent Mcl-1 transcription and inducing Akt/GSK3β-dependent protein degradation. J Cell Biochem. 2013; 114:1819-1831.
12. Kurosu T, Ohki M, Wu N, Kagechika H, Miura O. Sorafenib induces apoptosis specifically in cells expressing BCR/ABL by inhibiting its kinase activity to activate the intrinsic mitochondrial pathway. Cancer Res. 2009; 69:3927-3936.
13. Gauthier A, Ho M. Role of sorafenib in the treatment of advanced hepatocellular carcinoma: An update. Hepatol Res. 2013; 43:147-154.
14. Li G, Zhang S, Fang H, Yan B, Zhao Y, Feng L, Ma X, Ye X. Aspirin overcomes Navitoclax-resistance in hepatocellular carcinoma cells through suppression of Mcl-1. Biochem Biophys Res Commun. 2013; 434:809-814.
15. Wei W, Chua MS, Grepper S, So S. Small molecule antagonists of Tcf4/beta-catenin complex inhibit the growth of HCC cells *in vitro* and *in vivo*. Int J Cancer. 2010; 126:2426-2436.
16. Perkins ND. Integrating cell-signalling pathways with NF-κB and IKK function. Nat Rev Mol Cell Biol. 2007; 8:49-62.
17. Baldwin AS Jr. Series introduction: the transcription factor NF-kappaB and human disease. J Clin Invest. 2001; 107:3-6.
18. Wei Z, Doria C, Liu Y. Targeted therapies in the treatment of advanced hepatocellular carcinoma. Clin Med Insights Oncol. 2013; 7:87-102.
19. Zhang YS, Xie JZ, Zhong JL, Li YY, Wang RQ, Qin YZ, Lou HX, Gao ZH, Qu XJ. Acetyl-11-keto-β-boswellic acid (AKBA) inhibits human gastric carcinoma growth through modulation of the Wnt/β-catenin signaling pathway. Biochim Biophys Acta. 2013; 1830:3604-3615.
20. Wei Y, Shen N, Wang Z, Yang G, Yi B, Yang N, Qiu Y, Lu J. Sorafenib sensitizes hepatocellular carcinoma cell to cisplatin *via* suppression of Wnt/β-catenin signaling. Mol Cell Biochem. 2013; 381:139-144.
21. Inagaki Y, Tang W, Zhang L, Du GH, Xu WF, Kokudo N. Novel aminopeptidase N (APN/CD13) inhibitor 24F can suppress invasion of hepatocellular carcinoma cells as well as angiogenesis. Biosci Trends. 2010; 4:56-60.

(Received October 3, 2013; Revised October 12, 2013; Accepted October 15, 2013)